OPTIMIZATION TECHNOLOGY FOR NONLINEAR MICROWAVE CIRCUITS INTEGRATING ELECTROMAGNETIC SIMULATIONS

J.W. Bandler, R.M. Biernacki,
S.H. Chen and P.A. Grobelny

OSA-96-MM-3-R

March 5, 1996
(Revised August 2, 1996)

Optimization Technology for Nonlinear Microwave Circuits Integrating Electromagnetic Simulations

John W. Bandler,* Radoslaw M. Biernacki,* and Shao Hua Chen*

Optimization Systems Associates Inc., P.O. Box 8083, Dundas, Ontario, Canada L9H 5E7

Piotr A. Grobelny**

Newbridge Networks Corporation, Kanata, Ontario, Canada K2K 2E6

Received March 5, 1996; revised August 2, 1996.

ABSTRACT

We review relevant concepts, formulations and algorithms for microwave circuit optimization. Emphasis is given to recent advances in the state of the art: automated electromagnetic (EM) design, Space Mapping, Huber optimization, an integrated CAD environment and parallel computation. We address integration of previously disjoint simulation technologies for automated EM optimization of linear and nonlinear microwave circuits. We incorporate EM analyses of passive microstrip structures and SPICE models of active devices into harmonic balance optimization of nonlinear circuits, even for yield-driven design. Designs of a class B frequency doubler, a broad-band small-signal amplifier and an attenuator illustrate the integrated approach.

---

* Also affiliated with the Simulation Optimization Systems Research Laboratory and the Department of Electrical and Computer Engineering, McMaster University, Hamilton, Ontario, Canada L8S 4L7.

** Formerly affiliated with the Simulation Optimization Systems Research Laboratory and the Department of Electrical and Computer Engineering, McMaster University, Hamilton, Ontario, Canada L8S 4L7.

I. INTRODUCTION

Microwave circuit designers have become more enthusiastic and, while striving for first-pass success, more critical users of numerical optimization techniques in the [1]. Among their current needs and expectations for CAD tools are electromagnetic (EM) simulation (e.g., [2-9]), an integrated and concurrent design environment, mixed-domain multi-level hierarchical optimization, physical and physics-based modeling, intelligent and robust optimizers, yield and cost optimization, and visualization.

The thrust for faster and smaller circuits has raised EM field-theoretical studies to new prominence in the simulation of MMICs, interconnects, component packaging and housings, etc. However, the prevailing use of EM simulators for validation of designs obtained through traditional techniques does not fully exploit their predictive power. Furthermore, the widespread use of EM simulators for ad hoc design is highly wasteful of human and computer resources. We pioneered [10-15] direct and automated EM optimization with successful applications to designing matching circuits, filters, attenuators and amplifiers, including statistical analysis and yield optimization.

In EM optimization, the field solver, not the optimization algorithm, is the true bottleneck. This is especially significant when gradients are estimated by perturbations or when yield is estimated from many Monte Carlo outcomes. We promote parallel computing as an effective means of speeding up CPU intensive EM optimization [13].

Another challenge is to integrate optimization technology into a design environment with a diversified set of CAD tools, which may include digital, analog time-domain, analog frequency-domain, EM, mechanical and thermal simulators. Using the Datapipe technology [15] this can be achieved without immensely complicated syntax and protocols, e.g., [16]. We have developed a novel approach to capturing design data from external simulators in their native format which includes automated parameterization of arbitrary microstrip structures for EM optimization.

For nonlinear circuits, we integrate EM analyses with harmonic balance (HB) optimization [12]. For circuits containing active devices, we take advantage of the accurate EM models for passive components and the popular and time-tested SPICE models for active devices. The process of

invoking the two independent types of simulations and combining the results at the circuit level is automated to facilitate both nominal and statistical designs. Our work lays the software architectural foundation for a new generation of CAD systems with emphasis on the integration of heterogenous tools. The flexibility and benefits of this approach are illustrated by the design of two microwave circuits. The combination of EM simulation and HB optimization is demonstrated by a class B frequency doubler design. Nominal and statistical designs of a broad-band small-signal amplifier containing microstrip components exemplify the utilization of SPICE device models together with EM simulations. The numerical results were produced within the optimization environment of OSA90/hope [14] featuring a circuit-level HB simulator, connecting to the EM simulator *em* [7] through Empipe [14], and connecting to SPICE [17] through Spicepipe [18].

Our recent exploitation of Space Mapping (SM) [19, 20], a totally new concept in engineering optimization, has aroused great excitement. It opens new horizons of optimization linking engineering models of different types and levels of complexity, including empirical, EM-based, analytical, numerical, physics-based and even direct laboratory measurements, which represent the same physical design.

The SM concept is founded on the computational expediency of empirical engineering models (which embody expert knowledge accumulated over many years) and the acclaimed accuracy of EM simulators. SM facilitates automated design optimization within a practical time frame. We extended SM to parameter extraction and introduced the concept of Frequency Space Mapping (FSM) [20]. It provides a powerful means of overcoming problems of local minima and data misalignment, especially at the starting point.

In Section II we review relevant concepts, formulations and algorithms for microwave circuit optimization [21], including the novel approach to "robustizing" circuit optimization using Huber functions [22]. Section III provides a brief overview of direct EM optimization. Integration of HB and EM simulations [12] is presented in Sections IV and V, and incorporation of SPICE device models is discussed in Section VI. Space Mapping concepts are reviewed in Section VII. The resulting CAD environment is introduced in Section VIII, followed by applications presented in Sections IX-XI.

II. DESIGN OPTIMIZATION

We start by briefly reviewing the concepts involved in design optimization, including yield optimization. We formulate design as an abstract optimization problem, regardless of the nature of the object being designed. We show how the error functions for design goals are typically defined and discuss ways of combining them into a single objective function.

Design optimization is a powerful computational tool enabling designers to adjust designable parameters in order to meet design specifications. The nature of the designed object is irrelevant to the optimizer. However, the computer simulation of the object must be available. The computer simulator should provide the means for processing a number of input parameters, some of which are (directly or indirectly) designable, into the corresponding set of responses.

Simulation, Specifications and Error Functions

The response functions that can be of interest to the designer may involve a combination of frequency-domain responses, time-domain responses, space-domain responses, frequency spectra of periodic functions, and their functions such as power, etc. "Of interest" means that design specifications are imposed on the responses. A specification is typically imposed on a range of domain values. This leads to an infinite number of specifications and it becomes necessary to discretize the domain and consider only a finite subset of representative frequency, time or space points. After discretization, the jth specification can be denoted by S_{uj} or $S_{\ell j}$ if it is an upper or a lower specification, respectively.

In order to formulate an objective function for design optimization the object is simulated at the same frequency or time points at which the upper and/or lower specifications are selected by discretization. The corresponding responses are denoted by $R_j(\boldsymbol{x})$ and the error vector $\boldsymbol{e}(\boldsymbol{x})$ is defined as

$$\boldsymbol{e}(\boldsymbol{x}) = [e_1(\boldsymbol{x}) \;\; e_2(\boldsymbol{x}) \; . \; . \; . \; e_M(\boldsymbol{x})]^T \tag{1}$$

where the individual errors $e_j(\boldsymbol{x})$ are

$$e_j(\boldsymbol{x}) = w_j\,(R_j(\boldsymbol{x}) - S_{uj}) \quad \text{or} \quad e_j(\boldsymbol{x}) = w_j\,(S_{\ell j} - R_j(\boldsymbol{x})). \tag{2}$$

$\boldsymbol{x}$ is the vector of designable parameters, M is the total number of errors and w_j, $j = 1, 2, ..., M$, are non-negative weighting factors. The negative error values indicate that the corresponding specifications are satisfied. For positive error values the corresponding specifications are violated. The acceptability region $\boldsymbol{A}$ in the parameter space is defined as

$$\boldsymbol{A} = \left\{ \boldsymbol{x} \mid e_j(\boldsymbol{x}) < 0, \quad j = 1, 2, ..., M \right\} \tag{3}$$

Clearly, all specifications are satisfied if the designable parameters fall into $\boldsymbol{A}$, and at least one specification is violated if that point falls outside the acceptability region $\boldsymbol{A}$.

Objective Functions and Algorithms

For the purpose of optimization all the errors $e_j(\boldsymbol{x})$ have to be combined into a single objective function. Three important objective functions are minimax, ℓ_1 and ℓ_2 (least squares). The generalized ℓ_p function $U(\boldsymbol{x})$ from $e(\boldsymbol{x})$ takes the form [23, 24] (used, for example, in [25])

$$U(\boldsymbol{x}) = \begin{cases} \left[\sum\limits_{j \in \boldsymbol{J}} e_j(\boldsymbol{x})^p \right]^{1/p} & \text{if } \boldsymbol{x} \notin \boldsymbol{A} \\ -\left[\sum\limits_{j=1}^{M} \left(-e_j(\boldsymbol{x})\right)^{-p} \right]^{-1/p} & \text{if } \boldsymbol{x} \in \boldsymbol{A} \end{cases} \tag{4}$$

where $\boldsymbol{J} = \left\{ j \mid e_j(\boldsymbol{x}) \geq 0 \right\}$.

Some variations of this function include: (a) one-sided ℓ_p function where the lower expression in (4) is set to zero, and (b) the ℓ_p norm where only the upper expression in (4) is used and the summation is over the absolute values of e_j's for all $j = 1, 2, ..., M$. The minimax function corresponds to $p \rightarrow \infty$ and can simply be expressed as

$$U(\boldsymbol{x}) = \max_j \{e_j(\boldsymbol{x})\} \tag{5}$$

The novel Huber and one-sided Huber objectives combine respective advantages of ℓ_1 and ℓ_2. The Huber function is defined as [26]

$$\rho_k(e) = \begin{cases} e^2/2 & if\ |e| \le k \\ k|e| - k^2/2 & if\ |e| > k \end{cases} \tag{6}$$

where k is a positive constant threshold value and e represents an error function. The one-sided Huber function $\rho_k^+(x)$ [22] is defined similarly to all other one-sided functions by setting it to zero for negative error values. The Huber (or one-sided Huber) objective is simply defined as a sum of all Huber (or one-sided Huber) functions for all M errors.

Minimax is the objective of choice for performance-driven design optimization, aiming at equi-ripple solutions. The ℓ_2 norm or one-sided ℓ_2 function are also commonly used for performance-driven design optimization. The ℓ_1 and Huber functions are uniquely useful in modeling and in yield optimization. Exploiting the Huber functions we "robustize" circuit optimization [22]. Similarly to the ℓ_1 norm, the Huber function filters out gross errors and thus it automatically ignores "wild" measurement data points. On the other hand it treats small statistical variations and measurement errors in the smooth, least-squares sense. The Huber function is well suited to handle analog fault diagnosis problems.

Specialized algorithms exist for minimization of each of the aforementioned objective functions (e.g., [27]).

Yield Optimization

Yield optimization is an effective means of improving first-pass success in circuit design, e.g., [28-30]. Due to various fluctuations inherent in the manufacturing process, the circuit outcomes exhibit variations of their responses w.r.t the nominal design response. Manufacturing yield is simply the ratio of the number of circuit outcomes meeting all design specifications to the total number of outcomes. Formally, yield-driven optimization is formulated as

$$\underset{x^0}{maximize}\ \{\ Y(x^0) = \int_{R^n} I_a(x) f_x(x^0, x)\, dx\ \} \tag{7}$$

where $x^0 \in R^n$ is the vector of nominal circuit parameters, x is the vector of actual circuit outcome parameters, $f_x(x^0,x)$ is the probability density function (pdf) of x around x^0, $I_a(x) = 1$ if $x \in A$, and $I_a(x) = 0$ otherwise.

Since x is a continuous random variable an infinite number of outcomes would be involved in evaluating yield $Y(x^0)$ in (7) . Therefore, in practice a number of Monte Carlo outcomes, x^i, i = 1,2,...,K, is sampled around x^0 according to $f_x(x^0,x)$ and yield is estimated by

$$Y(x^0) \approx \frac{1}{K} \sum_{i=1}^{K} I_a(x^i) \tag{8}$$

The one-sided ℓ_1 objective function for yield-driven optimization is formulated as follows [1]. First, for each of K circuit outcomes x^i the corresponding error vector $e(x^i) = [e_1(x^i)\ e_2(x^i) \ldots e_M(x^i)]^T$ is determined from (2) with x replaced by x^i and the generalized ℓ_1 function (4), denoted here by $v(x^i)$, is calculated. This function has the property that it is positive if at least one specification is violated, i.e., $x^i \notin A$, and it is negative if all design specifications are satisfied. Then, the final one-sided ℓ_1 objective function is defined from $v(x^i)$ as

$$U(x^0) = \sum_{i \in J} \alpha_i v(x^i) \tag{9}$$

where J is defined similarly to (4) but w.r.t. $v(x^i)$. α_i are properly chosen positive multipliers. The function (9) naturally imitates the percentage of outcomes violating design specifications and, therefore, its minimization leads to yield improvement. An enhanced approach to yield optimization takes advantage of the yield probability function which replaces $v(x^i)$ in (9). A robust alternative to (9) is to formulate the yield optimization as a one-sided Huber problem.

Statistical Modeling

The purpose of statistical modeling is to determine or approximate the probability density function $f_x(x^0,x)$ in (7) from a sample of measurement data. Circuit simulation can be performed at different levels of primary parameters depending on available software tools or desired efficiency, e.g., timing

analysis, cell or device simulations. Therefore, the vector x^0 of designable parameters in (7) as well as the pdf must be considered at the same level as available or desired simulation. Physics-based and physical simulation (e.g., [30-32]) is the most suitable level for statistical device modeling.

We developed a statistical verification procedure for device models, using yield as the statistical estimator. Our new cumulative probability distribution fitting technique directly determines statistics such as the mean values and standard deviations in a single optimization [33].

Snowden noted in [32] that the advent of more powerful computers has increased the drive in using physical models and physics-based models for microwave and mm-wave CAD to meet the requirement of predictability and economization. Physical and physics-based models permit statistical characterization at the geometrical/process parameter level, and also offer the opportunity of device optimization. A methodology of integrating EM analyses of passive structures and physical simulations of active devices will have a tremendous impact on reducing the cost and time required for design cycles.

III. DIRECT EM OPTIMIZATION

We proposed direct and automated EM optimization with successful applications to designing matching circuits, filters, attenuators and amplifiers, including statistical analysis and yield optimization.

To successfully interface optimizers with EM simulators we needed to address a number of challenges that either did not exist or were not as severe in traditional simulators. This included efficiency, discretization of geometrical dimensions, and continuity of optimization variables. To effectively carry out direct EM optimization we introduced: (1) efficient on-line response interpolation w.r.t. geometrical dimensions of microstrip structures simulated with fixed grid sizes, (2) smooth and accurate gradient evaluation for use in conjunction with "geometrical" interpolation, and (3) storing the results of expensive EM simulations in a dynamically updated data base. Design optimization of a double folded stub bandstop filter and of a millimeter-wave 26-40 GHz interdigital capacitor bandpass microstrip filter illustrated the first applications of those techniques [11].

Our initial approach to direct EM optimization was by creating an element library (Empipe, OSA, 1992). It was designed specifically to interact with Sonnet's *em* and followed the conventional approach of predefined, built-in elements (primitives) such as lines, bends, junctions, gaps, stubs. Each element was already parameterized and ready for optimization. The circuits were decomposed into those predefined primitives. Although that approach gained immediate acceptance by CAD users, it inherently omits possible couplings between the elements since they are connected by the circuit-level simulator. Furthermore, it does not accommodate structures which cannot be decomposed into library elements.

One of the most attractive advantages of EM simulators is the ability to analyze structures of arbitrary geometry. Naturally, EM simulator users wish to be able to designate optimizable parameters directly within the graphical layout representation. To satisfy their wish, we must be able to relate geometrical coordinates of the layout to the numerical parameters for optimization. To automate such a parameterization process is quite a challenge.

Our new approach is based on the technique of Geometry Capture [15]. EM simulators deal directly with the layout representation of circuits in terms of absolute coordinates which are not directly designable parameters. Therefore, geometrical parameterization is needed for every new structure. Geometry Capture is a graphical tool for parameterizing arbitrary structures. It facilitates automatic translation of the values of user-defined designable parameters to the layout description in terms of absolute coordinates. During optimization, this translation is automatically performed for each new set of parameter values before the EM simulator is invoked.

IV. INTEGRATION OF EM AND HB SIMULATIONS

Large-signal circuit optimization with the HB technique has been significantly advanced during the last decade (e.g., [34-38]). The computational time has been greatly reduced due to the efficiency of the HB simulation and an elegant sensitivity calculation [36]. HB optimization using the FAST sensitivity technique has been applied to performance- and yield-driven designs [37, 38].

In HB, a nonlinear circuit is normally partitioned into a nonlinear subcircuit, a linear

subcircuit and an excitation subcircuit as shown in Fig. 1. Here, the linear subcircuit can be further divided into a lumped element subcircuit and a microstrip element subcircuit. Let the circuit parameters be

$$\phi = \left[\phi_N^T \; \phi_{LL}^T \; \phi_{LM}^T \right]^T \tag{10}$$

where ϕ_N are the parameters of the nonlinear subcircuit, ϕ_{LL} and ϕ_{LM} are the parameters of the lumped element subcircuit and the microstrip element subcircuit, respectively. The HB equation of the circuit is normally written as

$$F(\phi, V(\phi)) = I(\phi, V(\phi)) + j\Omega Q(\phi, V(\phi)) + Y(\phi)V(\phi) + I_s = 0 \tag{11}$$

where V is the vector of nonlinear port voltages to be solved for, I and Q the vectors of currents and charges entering the nonlinear ports, respectively, Ω the angular frequency matrix, I_s the vector of equivalent excitation currents, and Y the equivalent admittance matrix of the linear subcircuit corresponding to the connection ports. Incorporating the results of EM analysis of some linear subcircuits, Y is a function of frequency f and parameters of the linear subcircuit ϕ_{LL} and ϕ_{LM}, and can be expressed as

$$Y(\phi) = Y(f, \phi_{LL}, R_{EM}(f, \phi_{LM})) \tag{12}$$

where $R_{EM}(f, \phi_{LM})$ represents the EM responses.

Once $R_{EM}(f, \phi_{LM})$ is returned from the EM simulator $Y(\phi)$ is obtained from (12) and then the HB equation (11) is solved, typically by the Newton iteration.

V. INTEGRATED HB/EM GRADIENT-BASED OPTIMIZATION

Consider a vector of circuit responses

$$R_{CT}(\phi) = R(\phi, V(\phi, R_{EM}(\phi))) \tag{13}$$

which may include output voltages, currents, powers, power gains, etc. From these responses and the corresponding design specifications, we formulate an appropriate objective function, such as minimax, ℓ_1, ℓ_2 or Huber function, as discussed in Section II. For gradient-based optimization we need to calculate the derivatives of the circuit responses R_{CT} w.r.t. each design variable ϕ_i in ϕ.

$\partial R_{CT}/\partial \phi_i$ can be derived from (13) as

$$\frac{\partial R_{CT}}{\partial \phi_i} = \frac{\partial R}{\partial \phi_i} + \left[\frac{\partial R^T}{\partial V}\right]^T \left(\frac{\partial V}{\partial \phi_i} + \left[\frac{\partial V^T}{\partial R_{EM}}\right]^T \frac{\partial R_{EM}}{\partial \phi_i}\right) \tag{14}$$

which can be evaluated using an elegant gradient estimation technique [11].

The flowchart shown in Fig. 2 illustrates the established HB optimization augmented by EM simulations and thus outlines the complete HB/EM design optimization process.

VI. INTEGRATING SPICE DEVICE SIMULATION INTO HB/EM OPTIMIZATION

Capturing SPICE Device Models

The public domain SPICE program does not provide any means for optimization. Incorporating the results of EM simulations of passive subcircuits into SPICE requires an equivalent circuit representation and is not available in an automated fashion for optimization. The rigid structure of commercial versions of SPICE permits only limited optimization.

In order to incorporate SPICE simulation results into the overall design environment we developed a Datapipe based interface to OSA90/hope which we call Spicepipe [18]. The interface allows OSA90/hope to drive SPICE in an automated manner, with the SPICE input data determined in OSA90/hope and the SPICE results returned to OSA90/hope.

For the particular application of capturing SPICE device models, SPICE is invoked to simulate the device only. The SPICE output is returned to OSA90/hope and postprocessed, for example simulated node voltages are converted to the S parameters of the device (in fact, two SPICE simulations are carried out to determine the parameters of a 2-port network). Assuming that in addition to the nonlinear and the microstrip subcircuits there are m devices in the circuit, all to be simulated by SPICE, the overall circuit responses in (13) can now be expressed as

$$R_{CT}(\phi) = R(\phi, V(\phi, R_{EM}(\phi), R^1_{SP}(\phi), R^2_{SP}(\phi), ..., R^m_{SP}(\phi))) \tag{15}$$

where $R^1_{SP}(\phi)$, $R^2_{SP}(\phi)$, ..., $R^m_{SP}(\phi)$ are the SPICE simulated responses of the m device subcircuits.

Statistical Parameter Extraction with SPICE and OSA90/hope

Suppose there are n_d sets of data measured from n_d devices and n_i measured responses in the ith data set

$$S^i = [S^i_1 \; S^i_2 \; \ldots \; S^i_{n_i}]^T, \qquad i = 1, 2, \ldots, n_d \tag{16}$$

Corresponding to S^i we have the SPICE responses

$$R_{SP}(\phi^i) = [R_{SP_1}(\phi^i) \; R_{SP_2}(\phi^i) \; \ldots \; R_{SP_{n_i}}(\phi^i)]^T, \qquad i = 1, 2, \ldots, n_d \tag{17}$$

where ϕ^i is the ith set of model parameters to be extracted.

For each data set, the error vector (1), now expressed as

$$e_{OS}(\phi^i) = [e_{OS_1}(\phi^i) \; e_{OS_2}(\phi^i) \; \ldots \; e_{OS_{n_i}}(\phi^i)]^T \tag{18}$$

represents the equality constraints of the matching problem

$$e_{OS_j}(\phi^i) = R_{SP_j}(\phi^i) - S^i_j \tag{19}$$

The parameter extraction problem is then defined as

$$\underset{\phi^i}{\text{minimize}} \quad U_{OS}(\phi^i) \tag{20}$$

where U_{OS} is an objective function such as the ℓ_1, ℓ_2 or the Huber norm. For each device outcome the parameter extraction is driven by OSA90/hope's optimizer with the SPICE device model captured as described in the previous subsection. Repeated for each data set, this optimization leads to a sample of individually extracted device models. The model statistics including the mean values, standard deviations and the correlation matrix are then produced by postprocessing this sample of models using HarPE [14].

VII. SPACE MAPPING OPTIMIZATION

Space Mapping is a totally new concept in engineering optimization linking engineering models of different types and levels of complexity, including empirical, EM-based, analytical, numerical, physics-based and even direct laboratory measurements, which represent the same physical design. A key step in SM is to determine pairs of corresponding EM and empirical models through parameter extraction. The "empirical" model can even be a coarse EM simulation!

In its basic form, the SM optimization technique [19] exploits a mathematical link between input parameters of two simulators (models). One is considered very accurate but computationally very intensive while the other one is fast but less accurate. The goal is to direct the bulk of CPU intensive optimization to the fast model in the optimization system (OS) parameter space X_{OS}. This model is referred to as the OS simulator. EM simulations serve as the accurate model and the EM simulator input parameter space is denoted by X_{EM}. As a first step in SM optimization we carry out conventional design optimization entirely in the X_{OS} space. The resulting solution is denoted by x^*_{OS}. Then, we create and iteratively refine a mapping

$$x_{OS} = P(x_{EM}) \tag{21}$$

from X_{EM} to X_{OS} in order to align the two models.

In principle, the choice of the mathematical form of the mapping is an implementational issue. In [19] we only assume that the mapping can be expressed as a linear combination of some predefined and fixed fundamental functions. In the current implementation of SM we also assume that P is invertible. Once the mapping is established the inverse mapping P^{-1} is used to find the EM solution as the image of the optimal OS solution x^*_{OS}, namely,

$$\bar{x}_{EM} = P^{-1}(x^*_{OS}) \tag{22}$$

In other words, we map the optimal OS model parameters back into the EM parameters (e.g., physical layout).

P is established through an iterative process. The initial mapping $P^{(0)}$ is found using a preselected set B_{EM} of k points in X_{EM} and the set B_{OS} of corresponding points in X_{OS}. The number k of these base points should be sufficient to uniquely determine all the coefficients of the linear

combination defining the mapping. Their selection is fairly arbitrary. However, it is advantageous to select these points on the grid. The points in B_{OS} are determined by k auxiliary optimizations to achieve

$$f_{OS}(x^{i}_{OS}) \approx f_{EM}(x^{i}_{EM}), \quad i = 1, 2, ..., k \tag{23}$$

where f_{OS} and f_{EM} are the circuit responses simulated by the OS and EM simulators, respectively. This may be referred to as a parameter extraction (fit). In other words, we optimize the OS model to fit its response to the EM simulator response calculated at x^{i}_{EM}. In this optimization the OS model parameters x_{OS} are the optimization variables. As a result we find the point x^{i}_{OS}. This process is repeated for all the base points.

At the jth iteration B_{EM} is expanded by the new image of x^{*}_{OS} computed using (22) where the current approximation to the mapping is used in place of P. The iterations continue until

$$\| f_{EM}(\bar{x}_{EM}) - f_{OS}(x^{*}_{OS}) \| \leq \epsilon \tag{24}$$

where $\|\cdot\|$ indicates a suitable norm and ϵ is a small positive constant. Otherwise, another parameter extraction is carried out, B_{OS} is expanded accordingly and the approximation to the mapping is updated.

Recently, we proposed a new aggressive SM strategy [20]. Instead of waiting for upfront EM analyses at several base points, it exploits every available EM analysis, producing dramatic results right from the first step. We assume that the mapping P can be linearized locally, such that at the jth iteration we have

$$P(x^{(j)}_{EM} + h) \approx P(x^{(j)}_{EM}) + A^{(j)} h. \tag{25}$$

We target every EM analysis at the optimal design in the sense that $x^{(j)}_{EM}$ is generated not merely as a base point for establishing the mapping, but as our current best estimate of the mapped solution as defined by (21). The mapping P is found iteratively starting from $P^{(0)}(x) = x$.

At the starting point we let $x^{(1)}_{EM} = x^{*}_{OS}$ and $A^{(1)} = 1$. At the jth iteration, we obtain $x^{(j+1)}_{EM}$ by applying (22) using the current estimate of P, namely $P^{(j)}$. If the EM analysis at $x^{(j+1)}_{EM}$ produces

the desired responses, then our mission is accomplished. Otherwise, we find $x_{OS}^{(j+1)}$ which corresponds to $x_{EM}^{(j+1)}$ by parameter extraction, i.e., we extract $x_{OS}^{(j+1)}$ through optimization in X_{OS} from the data provided by the EM analysis at $x_{EM}^{(j+1)}$.

Adapting the Broyden formula [39], we update the SM transformation by

$$A^{(j+1)} = A^{(j)} + \frac{[x_{OS}^{(j+1)} - x_{OS}^{*}]h^{(j)T}}{h^{(j)T}h^{(j)}} \tag{26}$$

where $h^{(j)} = x_{EM}^{(j+1)} - x_{EM}^{(j)}$.

Frequency Space Mapping

As one of the key steps of SM we need to extract the parameter values of the corresponding empirical model such that it would match the EM simulation results. The uniqueness of the parameter extraction phase is of utmost importance to the success of SM. This can be a serious challenge, especially at the starting point, when the responses produced by EM analysis and by the empirical model may be severely misaligned, such as the case shown in Fig. 3. If we perform straightforward optimization from such a starting point, the extraction process can be trapped by a local minimum, as illustrated in Fig. 4.

We discovered a method for applying SM to parameter extraction and introduced the concept of automated Frequency Space Mapping (FSM) [20]. It leads to a powerful means of overcoming problems of local minima and data misalignment.

The mapping can be as simple as frequency shift and scaling. We proposed two algorithms for FSM: a sequential FSM algorithm (SFSM) and an exact penalty function (EPF) algorithm [20]. The initial mapping is determined by optimizing the mapping coefficients while the circuit parameters are kept fixed. In SFSM, we perform a sequence of parameter extraction optimizations in which the FSM is gradually reduced to the identity mapping. In the EPF algorithm, we perform only one optimization, but a sensible selection of the weighting factors is needed.

VIII. CAD DESIGN ENVIRONMENT

For advances in optimization technology to benefit a large number of CAD users, such advances have to be integrated into a design environment with a diversified set of CAD tools, which may include digital, analog time-domain, analog frequency-domain, EM, mechanical and thermal simulators. Efficiency of the algorithms as well as organization of software are of utmost importance. Software modularity must be facilitated and modules of different origin need to be accommodated. For example, advanced, state-of-the-art optimization routines must interact with field simulators, developed separately, possibly in a different language and without optimization as the objective.

Our Datapipe makes such integration easy and flexible. It is based on the technique called IPPC (inter-program pipe communication) which allows for high speed numerical interaction between independent programs. Datapipe consists of a number of ready-to-use communication protocols, and only a small file server needs to be attached to an external module in order to make it pipe-ready, thus becoming integrated into the CAD design environment. For encapsulated external simulators we have developed a novel approach to capturing design data in their native format.

Fig. 5 depicts the optimization environment incorporating the Sonnet *em* simulator and SPICE device models. In this environment Geometry Capture for arbitrary microstrip structures complements the Empipe library of typical primitives.

We promote parallel computing as an effective means of speeding up CPU intensive EM optimization [13]. The general concept of parallel computing can be realized in many different ways, including multiprocessor computers and specialized compilers. However, parallel computing does not necessarily require an expensive multiprocessor system. It can be realized by distributing the computational load over a network of heterogeneous computers. We rely on standard UNIX protocols (remote shell and equivalent hosts) instead of any platform specific mechanisms. This allows us to apply the concept to both local and wide area networks of heterogeneous workstations.

We chose to split the load of EM analyses on the component/subcircuit level for two reasons: to reduce the complexity of implementation and to best suit the operational flow of interpolation, optimization and statistical analysis. For instance, if the parameter values are off the mesh grid

imposed by the EM simulator, a number of EM analyses are needed at adjacent on-grid points for interpolation. In order to estimate the gradients for optimization, a number of perturbed analyses are required in addition to the analysis at the nominal point. For statistical analysis, EM analyses are to be performed at many Monte Carlo outcomes. By carrying out these analyses in parallel, the overall simulation time can be reduced by a factor of n, where n denotes the ratio between the combined effective computing power of the networked computers and that of a single computer (assuming that the overhead of parallelization is negligible compared with the CPU-intensive EM analyses).

The distribution of computational load is organized on one of the networked computers (master host). Using the UNIX remote shell command, an EM analysis is started on each of the available hosts. When the analysis is finished on a host, the next job, if any, is dispatched to that host. We can further improve the efficiency by combining parallelization with data interpolation and response function modeling. The EM simulation results are gathered from all the hosts and stored in a data base created on the master host. Fig. 6 illustrates this mechanism.

IX. SIMULATION AND OPTIMIZATION OF A CLASS B FREQUENCY DOUBLER

A class B frequency doubler is used as an example to demonstrate integrated HB/EM simulation and optimization. The circuit structure, shown in Fig. 7, follows [40, 12]. It consists of a single FET (NE71000) and a number of distributed microstrip elements including two radial stubs and two large bias pads.

Significant couplings between the distributed microstrip elements exist in this circuit, e.g., the couplings between the radial stubs and the bias pads. The conventional approach using empirical or physical models for individual microstrip elements neglects these couplings and therefore may result in large response errors. In order to take into account these couplings the entire microstrip structure should be considered as a single element to be simulated and optimized.

The design specifications are

conversion gain $\geq$ 3 dB

spectral purity $\geq$ 20 dB

at 7 GHz and 10 dBm input power.

We use the Curtice and Ettenberg FET model [41] to model the FET NE71000. The model parameters are extracted from the typical DC and S parameters [42] using HarPE [14]. The entire microstrip structure between the two capacitors (see Fig. 7) is parameterized using Geometry Capture and considered as one element to be simulated by *em*. The results are directly returned to OSA90/hope through Empipe for HB simulation and optimization. Ten parameters denoted as ϕ_1, ϕ_2, ..., ϕ_{10} are selected as design variables. It is worth pointing out, that the HB analysis requires the DC S parameters which are not generated by *em*, and thus must be separately provided. The minimax optimizer of OSA90/hope directs the performance-driven design. The values of the design variables before and after optimization are listed in Table I. The conversion gain versus input power before and after optimization is shown in Fig. 8. The source and output voltage waveforms before and after optimization are plotted in Fig. 9. The 3D view of conversion gain versus frequency and input power before and after optimization are shown in Fig. 10. Significant improvement of the circuit performance is obtained and all specifications are satisfied after optimization.

X. NOMINAL AND STATISTICAL DESIGN OF A SMALL-SIGNAL AMPLIFIER

To illustrate design utilizing simultaneously EM simulations and SPICE device modeling we consider a broadband small-signal amplifier with microstrip components [10] as shown in Fig. 11. The specification is

$$7 \text{ dB} \le |S_{21}| \le 8 \text{ dB} \quad \text{for} \quad 6 \text{ GHz} \le f \le 18 \text{ GHz}$$

where f is the frequency. The microstrip components are accurately simulated by *em* utilizing the line and the T-structure primitives of the Empipe [14] library. The MESFET is simulated by SPICE using the model shown in Fig. 12. There are 18 model parameters. The parameter statistics have been extracted from the synthetic data generated by Monte Carlo simulation using the model given in [10] and include the mean values, standard deviations, discrete density functions (DDF) and correlation matrix. The parameter mean values and standard deviations are listed in Table II. The circuit-level simulation and optimization are carried out by OSA90/hope.

Each of the microstrip T-structures is defined by six geometrical parameters and the feedback microstrip line is defined by two geometrical parameters, as shown in Fig. 13. Following [10], we choose W_{g1}, L_{g1}, W_{g2}, L_{g2} of the gate T-structure and W_{d1}, L_{d1}, W_{d2}, L_{d2} of the drain T-structure as design variables. W_{g3}, L_{g3}, W_{d3} and L_{d3} of the T-structures, W and L of the feedback microstrip line, as well as the MESFET parameters are not optimized. The small-signal gain before and after nominal optimization are plotted in Fig. 14.

For statistical design we assume a uniform distribution with 0.5 mil tolerance for all geometrical parameters. Yield at the nominal minimax solution is 43%. It is increased to 74% after yield optimization, which was performed using 50 outcomes. Fig. 15 shows the run charts before and after yield optimization for all of the 250 outcomes used in yield estimations at the frequency of 18 GHz. Clearly, many more outcomes meet the specification on $|S_{21}|$ after yield optimization. Table III lists values of the geometrical parameters at the nominal minimax solution and at the centered design.

XI. STATISTICAL DESIGN OF A 10 DB DISTRIBUTED ATTENUATOR

Consider the distributed attenuator depicted in Fig. 16 [13]. The 15 mil substrate has a relative dielectric constant of 9.8. It exemplifies structures which are difficult, if not impossible, to be decomposed into library primitives. We treat the attenuator as one piece and define 8 geometrical parameters for Geometry Capture, namely P_1, P_2, ..., P_8. P_1, P_2, P_3 and P_4 are assumed to be designable parameters. EM simulation of the attenuator at a single frequency requires about 7 CPU minutes on a Sun SPARCstation 1+. The design specifications are given as

$$9.5 \text{ dB} \leq \text{insertion loss} \leq 10.5 \text{ dB from 2 GHz to 18 GHz}$$

$$\text{return loss} \geq 10 \text{ dB from 2 GHz to 18 GHz}$$

The error functions are calculated at three frequencies: 2, 10 and 18 GHz.

First, we obtain a nominal design by minimax optimization. It requires 30 EM analyses. The nominal design took about 168 minutes on the network of Sun SPARCstations 1+.

For statistical design we assume normal distributions with a standard deviation of 0.25 mil for

all 8 geometrical parameters. Estimated from 250 Monte Carlo outcomes, the yield is 82% at the minimax nominal solution. The yield is increased to 97% after design centering. The statistical simulation and optimization called for 113 additional EM analyses. Fig. 17 shows the Monte Carlo sweep of the attenuator responses.

XII. CONCLUSIONS

We have reviewed a number of concepts which are critical to the successful application of optimization technology to microwave circuit modeling and design. Space Mapping is one of the most exciting concepts we have ever discovered. SM has already had a tremendous impact on automated EM optimization. The expansion of SM to hierarchically structured, optimization-oriented, CAD systems promises to integrate optimization technology with field theory, circuit theory and system theory based simulators for process-oriented linear, nonlinear and statistical CAD. We are convinced that CAD and modeling of engineering devices, circuits and systems will reach a level of precision and computational efficiency previously undreamed of. We have discussed issues related to an integrated approach to EM optimization of linear and nonlinear microwave and millimeter-wave circuits. The goal is to handle new applications such as investigating new microstrip components and to accurately design circuits consisting of complicated structures.

For the first time, we have integrated EM simulations directly with nonlinear HB simulation and optimization. We have also combined accurate EM models of passive microstrip structures with SPICE device models for nominal and statistical optimization. This approach has been demonstrated through the optimization of a class B frequency doubler as well as the nominal and statistical designs of a broad-band small-signal amplifier.

There are many other promising developments in microwave circuit optimization, e.g., [43]. One aspect in urgent need of attention is an accepted set of benchmark standards for comparing the accuracy, efficiency and robustness of different optimization techniques and methods. The establishment of such standards will contribute greatly to the understanding of the strength and weakness of optimization technology by microwave engineers at large.

ACKNOWLEDGEMENTS

Continued interaction with Dr. K. Madsen of the Technical University of Denmark, Dr. J.C. Rautio, President of Sonnet Software, Inc. and D.G. Swanson, Jr., of Watkins-Johnson Company is greatly appreciated. The authors would like to thank Mr. R.H. Hemmers and Dr. Q. Cai who contributed to some developments described in this paper. This work was supported in part by Optimization Systems Associates Inc. and in part by the Natural Sciences and Engineering Research Council of Canada under Grants OGP0007239, OGP0042444, STR0167080 and through the Micronet Network of Centres of Excellence.

REFERENCES

1. J.W. Bandler and S.H. Chen, "Circuit optimization: the state of the art," *IEEE Trans. Microwave Theory Tech.*, vol. 36, 1988, pp. 424-443.

2. J.C. Rautio and R.F. Harrington, "An electromagnetic time-harmonic analysis of arbitrary microstrip circuits," *IEEE Trans. Microwave Theory Tech.*, vol. 35, 1987, pp. 726-730.

3. R.H. Jansen and P. Pogatzki, "A hierarchically structured, comprehensive CAD system for field theory-based linear and nonlinear MIC/MMIC design," *1992 2nd Int. Workshop of the German IEEE MTT/AP Joint Chapter on Integrated Nonlinear Microwave and Millimeterwave Circuits Dig.* (Duisburg, Germany), 1992, pp. 333-341.

4. *LINMIC+/N Version 3.0*, Jansen Microwave, Bürohaus am See, Am Brüll 17, D-4030 Ratingen 1, Germany, 1992.

5. W.J.R. Hoefer, "Time domain electromagnetic simulation for microwave CAD applications," *IEEE Trans. Microwave Theory Tech.*, vol. 40, 1992, pp. 1517-1527.

6. V.J. Brankovic, D.V. Krupezevic and F. Arndt, "Efficient full-wave 3D and 2D waveguide eigenvalue analysis by using the direct FD-TD wave equation formulation," *IEEE MTT-S Int. Microwave Symp. Dig.* (Atlanta, GA), 1993, pp. 897-900.

7. ***em***™ and ***xgeom***™, Sonnet Software, Inc., 1020 Seventh North Street, Suite 210, Liverpool, NY 13088.

8. F. Alessandri, M. Dionigi, R. Sorrentino and M. Mongiardo, "A fullwave CAD tool of waveguide components using a high speed direct optimizer," *IEEE MTT-S Int. Microwave Symp. Dig.* (San Diego, CA), 1994, pp. 1539-1542.

9. D.G. Swanson, Jr., "Using a microstrip bandpass filter to compare different circuit analysis techniques," *Int. J. Microwave and Millimeter-Wave Computer-Aided Engineering*, vol. 5, 1995, pp. 4-12.

10. J.W. Bandler, R.M. Biernacki, S.H. Chen, P.A. Grobelny and S. Ye, "Yield-driven electromagnetic optimization via multilevel multidimensional models," *IEEE Trans. Microwave Theory Tech.*, vol. 41, 1993, pp. 2269-2278.

11. J.W. Bandler, R.M. Biernacki, S.H. Chen, D.G. Swanson, Jr. and S. Ye, "Microstrip filter design using direct EM field simulation," *IEEE Trans. Microwave Theory Tech.*, vol. 42, 1994, pp. 1353-1359.

12. J.W. Bandler, R.M. Biernacki, Q. Cai, S.H. Chen and P.A. Grobelny, "Integrated harmonic balance and electromagnetic optimization with Geometry Capture," *IEEE MTT-S Int. Microwave Symp. Digest* (Orlando, FL), 1995, pp. 793-796.

13. J.W. Bandler, R.M. Biernacki, Q. Cai, S.H. Chen, P.A. Grobelny and D.G. Swanson, Jr., "Heterogeneous parallel yield-driven electromagnetic CAD," *IEEE MTT-S Int. Microwave Symp. Dig.* (Orlando, FL), 1995, pp. 1085-1088.

14. *OSA90/hope*™, *Empipe*™ and *HarPE*™, Optimization Systems Associates Inc., P.O. Box 8083, Dundas, Ontario, Canada L9H 5E7.

15. Datapipe and Geometry Capture are trademarks of Optimization Systems Associates Inc., P.O. Box 8083, Dundas, Ontario, Canada L9H 5E7.

16. P.P.M. So, W.J.R. Hoefer, J.W. Bandler, R.M. Biernacki and S.H. Chen, "Hybrid frequency/time domain field theory based CAD of microwave circuits," *Proc. 23rd European Microwave Conf.*, (Madrid, Spain), 1993, pp. 218-219.

17. T. Quarles, A.R. Newton, D.O. Pederson and A. Sangiovanni-Vincentelli, *SPICE3 Version 3f4 User's Manual*. Department of Electrical Engineering and Computer Sciences, University of California, Berkeley, CA, 1993.

18. *Spicepipe*™, Research Version, Optimization Systems Associates Inc., P.O. Box 8083, Dundas, Ontario, Canada L9H 5E7, 1994.

19. J.W. Bandler, R.M. Biernacki, S.H. Chen, P.A. Grobelny and R.H. Hemmers, "Space mapping technique for electromagnetic optimization," *IEEE Trans. Microwave Theory Tech.*, vol. 42, 1994, pp. 2536-2544.

20. J.W. Bandler, R.M. Biernacki, S.H. Chen, R.H. Hemmers and K. Madsen, "Aggressive space mapping for electromagnetic design," *IEEE MTT-S Int. Microwave Symp. Dig.* (Orlando, FL), 1995, pp. 1455-1458.

21. J.W. Bandler, R.M. Biernacki and S.H. Chen, "Optimization technology for microwave circuit modeling and design," *Proc. 25th European Microwave Conf.* (Bologna, Italy), 1995, pp. 101-108.

22. J.W. Bandler, S.H. Chen, R.M. Biernacki, L. Gao, K. Madsen and H. Yu, "Huber optimization of circuits: a robust approach," *IEEE Trans. Microwave Theory Tech.*, vol. 41, 1993, pp. 2279-2287.

23. J.W. Bandler and C. Charalambous, "Practical least pth optimization of networks," *IEEE Trans. Microwave Theory Tech.*, vol. MTT-20, 1972, pp. 834-840.

24. C. Charalambous, "Nonlinear least pth optimization and nonlinear programming," *Math. Programming*, vol. 12, 1977, pp. 195-225.

25. V. Rizzoli, A. Costanzo and C. Cecchetti, "Numerical optimization of microwave oscillators and VCOs," *IEEE MTT-S Int. Microwave Symp. Dig.* (Atlanta, GA), 1993, pp. 629-632.

26. P. Huber, *Robust Statistics*. New York: Wiley, 1981.

27. J. Hald and K. Madsen, "Combined LP and quasi-Newton methods for minimax optimization," *Math. Programming*, vol. 20, 1981, pp. 49-62.

28. K. Singhal and J.F. Pinel, "Statistical design centering and tolerancing using parametric sampling," *IEEE Trans. Circuits and Systems*, vol. CAS-28, 1981, pp. 692-701.

29. E.M. Bastida, G.P. Donzelli and M. Pagani, "Efficient development of mass producible MMIC circuits," *IEEE Trans. Microwave Theory Tech.*, vol. 40, 1992, pp. 1364-1373.

30. D.E. Stoneking, G.L. Bilbro, P.A. Gilmore, R.J. Trew and C.T. Kelley, "Yield optimization using a GaAs process simulator coupled to a physical device model," *IEEE Trans. Microwave Theory Tech.*, vol. 40, 1992, pp. 1353-1363.

31. F. Filicori, G. Ghione and C.U. Naldi, "Physics-based electron device modelling and computer-aided MMIC design," *IEEE Trans. Microwave Theory Tech.*, vol. 40, 1992, pp. 1333-1352.

32. C.M. Snowden, "Nonlinear modelling of power FETs and HBTs," *Third Int. Workshop on Integrated Nonlinear Microwave and Millimeterwave Circuits INMMC'94, Digest* (Duisburg, Germany), 1994, pp. 11-25.

33. J.W. Bandler, R.M. Biernacki, Q. Cai and S.H. Chen, "Device statistical modelling and verification," *Microwave Engineering Europe*, May 1995, pp. 35-41.

34. V. Rizzoli, A. Lipparini and E. Marazzi, "A general-purpose program for nonlinear microwave circuit design," *IEEE Trans. Microwave Theory Tech.*, vol. 31, 1983, pp. 762-770.

35. K.S. Kundert and A. Sangiovanni-Vincentelli, "Simulation of nonlinear circuits in the frequency domain," *IEEE Trans. Computer-Aided Design*, vol. CAD-5, 1986, pp. 521-535.

36. J.W. Bandler, Q.J. Zhang and R.M. Biernacki, "A unified theory for frequency-domain simulation and sensitivity analysis of linear and nonlinear circuits," *IEEE Trans. Microwave Theory Tech.*, vol. 36, 1988, pp. 1661-1669.

37. J.W. Bandler, Q.J. Zhang, J. Song and R.M. Biernacki, "FAST gradient based yield optimization of nonlinear circuits," *IEEE Trans. Microwave Theory Tech.*, vol. 38, 1990, pp. 1701-1710.

38. J.W. Bandler, R.M. Biernacki, Q. Cai, S.H. Chen, S. Ye and Q.J. Zhang, "Integrated physics-oriented statistical modeling, simulation and optimization," *IEEE Trans. Microwave Theory Tech.*, vol. 40, 1992, pp. 1374-1400.

39. C.G. Broyden, "A class of methods for solving nonlinear simultaneous equations," *Math. of Comp.*, vol. 19, 1965, pp. 577-593.

40. "CAD review: the 7GHz doubler circuit," *Microwave Engineering Europe*, May 1994, pp. 43-53.

41. W.R. Curtice and M. Ettenberg, "A nonlinear GaAs FET model for use in the design of output circuits for power amplifiers," *IEEE Trans. Microwave Theory Tech.*, vol. MTT-33, 1985, pp. 1383-1394.

42. "RF and Microwave Semiconductors," *NEC Data Book*, NEC California Eastern Laboratories, 1994.

43. V. Rizzoli, A. Costanzo, F. Mastri and C. Cecchetti, "Harmonic-balance optimization of microwave oscillators for electrical performance, steady-state stability, and near-carrier phase noise," *IEEE MTT-S Int. Microwave Symp. Dig.* (San Diego, CA), 1994, pp. 1401-1404.

Figure Captions

Figure 1. Partition of a nonlinear microwave circuit for combined HB/EM simulation.

Figure 2. Flowchart of integrated EM/HB circuit design optimization.

Figure 3. An example of a response simulated using an empirical model (——) and ***em*** (---) at the starting point for parameter extraction.

Figure 4. Visualization of the ℓ_1 norm versus two of the model parameters L_2 and L_3, superimposed by the trace of the straightforward ℓ_1 optimization. The optimization converged to a local minimum instead of the true solution represented by the valley near the front of the graph.

Figure 5. EM optimization environment combining OSA90/hope's design simulation and optimization with Geometry Capture for arbitrary structures, the Empipe library of typical microstrip primitives and SPICE device modeling.

Figure 6. Parallel computing by distributing EM analyses over a network of computers.

Figure 7. Circuit structure of the class B frequency doubler.

Figure 8. Conversion gain of the frequency doubler versus input power before and after optimization.

Figure 9. Source and output voltage waveforms of the frequency doubler before and after optimization.

Figure 10. 3D view of conversion gain of the frequency doubler versus input power and frequency, (a) before and (b) after optimization.

Figure 11. Broad-band small-signal amplifier with microstrip components.

Figure 12. Equivalent circuit for the SPICE MESFET model.

Figure 13. Parameters of the feedback microstrip line and the microstrip T-structures.

Figure 14. $|S_{21}|$ response of the broad-band small-signal amplifier before (---) and after (——) nominal minimax design.

Figure 15. Run charts of the $|S_{21}|$ response of the broad-band small-signal amplifier at 18 GHz (a) before and (b) after yield optimization. 250 outcomes are used.

Figure 16. 10 dB distributed attenuator. The shaded T area corresponds to metallization of a high resistivity (50 Ω/sq) and the feed lines and the grounding pad are assumed to be lossless.

Figure 17. Monte Carlo sweeps of the attenuator insertion loss (——) and return loss (---) after yield optimization.

Bandler *et al.* "Optimization Technology ...", **Table I**

International Journal of Microwave and Millimeter-Wave Computer-Aided Engineering, vol. 7, no. 1, January 1997, Special Issue on Optimization-Oriented Microwave CAD.

TABLE I

FREQUENCY DOUBLER:
DESIGN VARIABLE VALUES
BEFORE AND AFTER MINIMAX OPTIMIZATION

Variable	Before Optimization	After Optimization
ϕ_1	1.5	1.494
ϕ_2	8.1	7.820
ϕ_3	3.3	3.347
ϕ_4	5.7	5.992
ϕ_5	2.4	2.550
ϕ_6	2.4	2.305
ϕ_7	1.8	1.750
ϕ_8	7.8	7.827
ϕ_9	4.2	4.242
ϕ_{10}	2.7	2.622

All dimensions are in mm.

International Journal of Microwave and Millimeter-Wave Computer-Aided Engineering, vol. 7, no. 1, January 1997, Special Issue on Optimization-Oriented Microwave CAD.

TABLE II

PARAMETER MEAN VALUES AND
STANDARD DEVIATIONS OF
THE STATISTICAL SPICE MESFET MODEL

Parameter	Mean	Standard Deviation (%)
C_{gs} (pF)	0.712	2.76
C_{gd} (pF)	0.032	1.79
λ (1/V)	0.297×10^{-3}	3.77
V_{to} (V)	-4.363	2.31
β (A/V^2)	0.0139	2.37
B (1/V)	2.85×10^{-3}	4.08
α (1/V)	1.916	4.04
R_d (Ω)	0.0692	4.03
R_s (Ω)	7.047	1.52
PB (V)	0.186	4.01
R_g (Ω)	1.988	3.56
G_{ds} (1/Ω)	4×10^{-3}	2.56
C_{ds} (pF)	0.055	1.59
L_g (nH)	0.0076	3.93
L_d (nH)	0.0127	3.46
L_s (nH)	0.104	3.47
C_{ge} (pF)	0.0819	2.75
C_x (pF)	20.0	-

Parameters C_{gs} through PB are the intrinsic SPICE MESFET parameters [13]. Parameters R_g through C_x are the extrinsic parameters (see Fig. 12). C_x is assumed non-statistical.

International Journal of Microwave and Millimeter-Wave Computer-Aided Engineering, vol. 7, no. 1, January 1997, Special Issue on Optimization-Oriented Microwave CAD.

TABLE III

MICROSTRIP PARAMETERS
FOR THE SMALL-SIGNAL AMPLIFIER

Parameter (mil)	Nominal solution	Centered solution
W_{g1}	15.975	14.688
L_{g1}	33.517	38.316
W_{g2}	7.980	8.265
L_{g2}	26.807	28.244
W_{d1}	4.980	4.882
L_{d1}	6.005	8.436
W_{d2}	2.687	2.051
L_{d2}	14.320	19.015

Only the optimized parameters are listed.

The subscripts g and d denote the parameters of the gate and drain T-structures, respectively (see Figs. 11 and 13).

Bandler *et al.* "Optimization Technology ...", **Figure 1**

International Journal of Microwave and Millimeter-Wave Computer-Aided Engineering, vol. 7, no. 1, January 1997, Special Issue on Optimization-Oriented Microwave CAD.

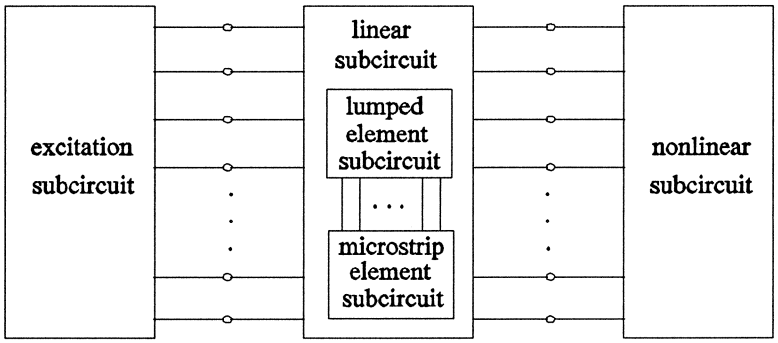

Bandler *et al.* "Optimization Technology ...", **Figure 2**

International Journal of Microwave and Millimeter-Wave Computer-Aided Engineering, vol. 7, no. 1, January 1997, Special Issue on Optimization-Oriented Microwave CAD.

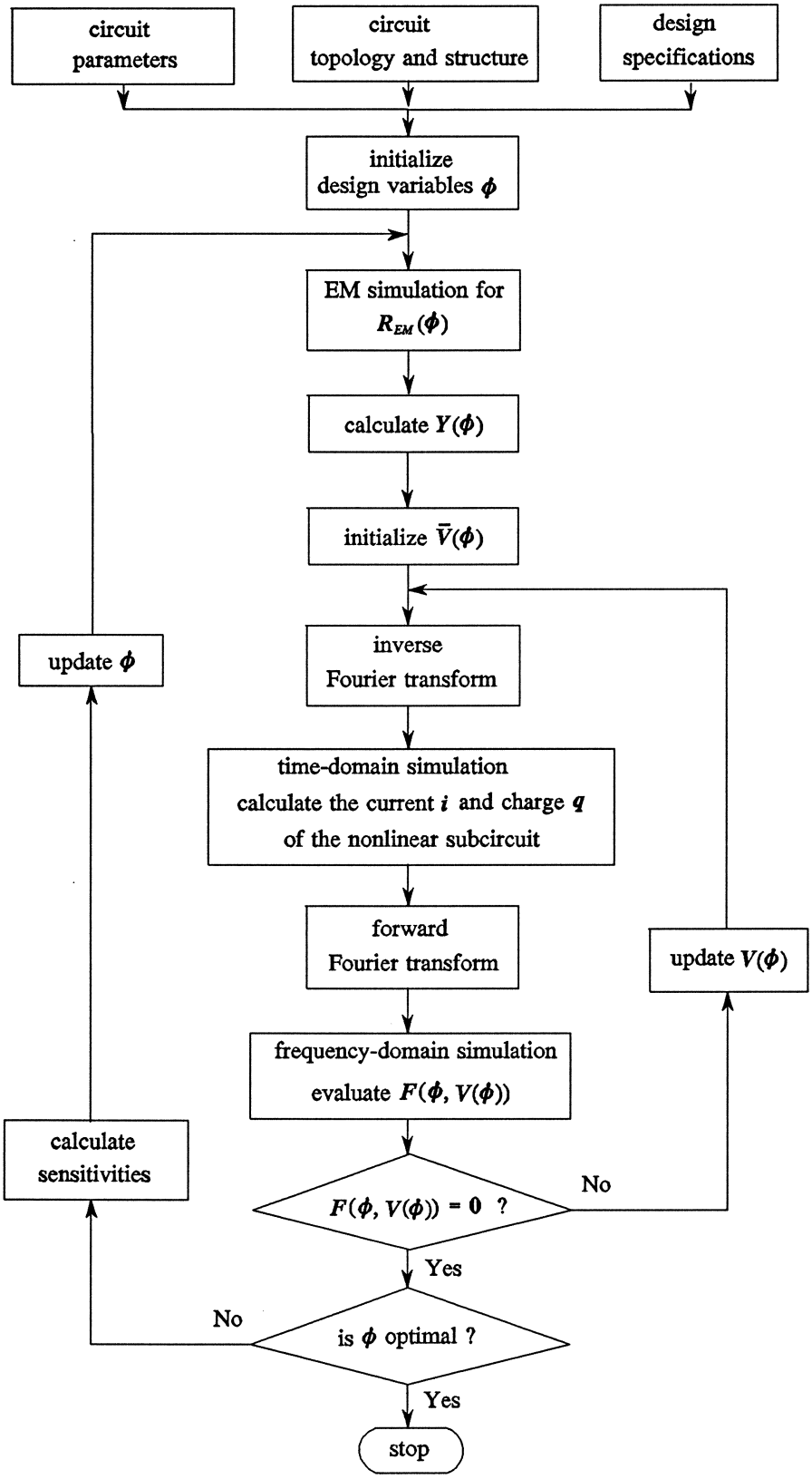

Bandler *et al.* "Optimization Technology ...", **Figure 3**

International Journal of Microwave and Millimeter-Wave Computer-Aided Engineering, vol. 7, no. 1, January 1997, Special Issue on Optimization-Oriented Microwave CAD.

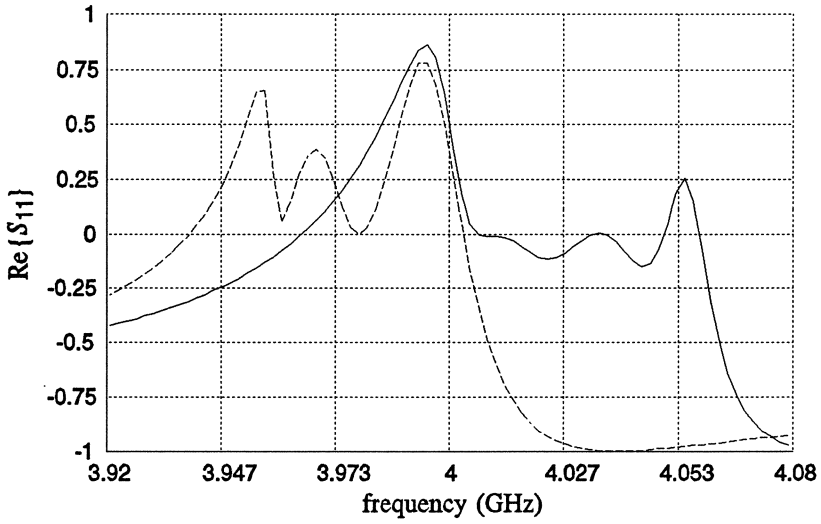

Bandler *et al.* "Optimization Technology ...", **Figure 4**

International Journal of Microwave and Millimeter-Wave Computer-Aided Engineering, vol. 7, no. 1, January 1997, Special Issue on Optimization-Oriented Microwave CAD.

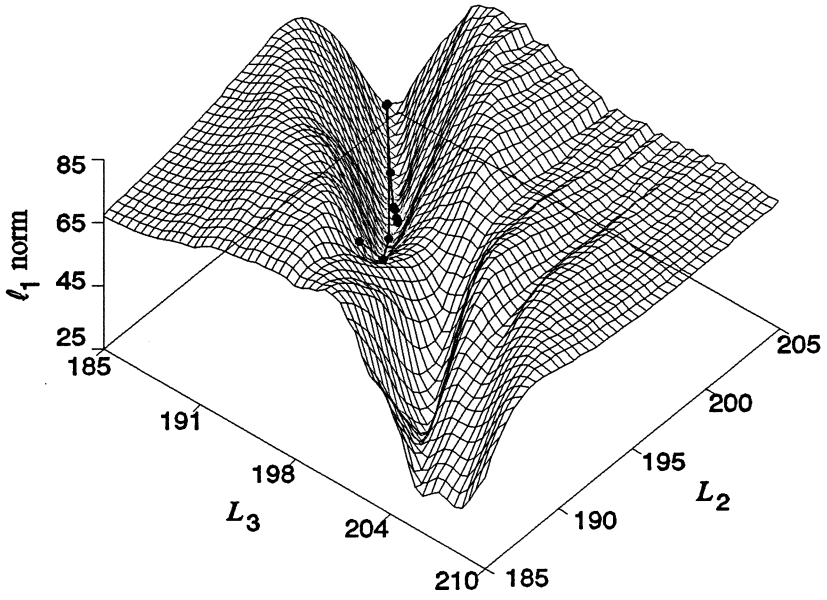

Bandler *et al.* "Optimization Technology ...", **Figure 5**
International Journal of Microwave and Millimeter-Wave Computer-Aided Engineering, vol. 7, no. 1, January 1997, Special Issue on Optimization-Oriented Microwave CAD.

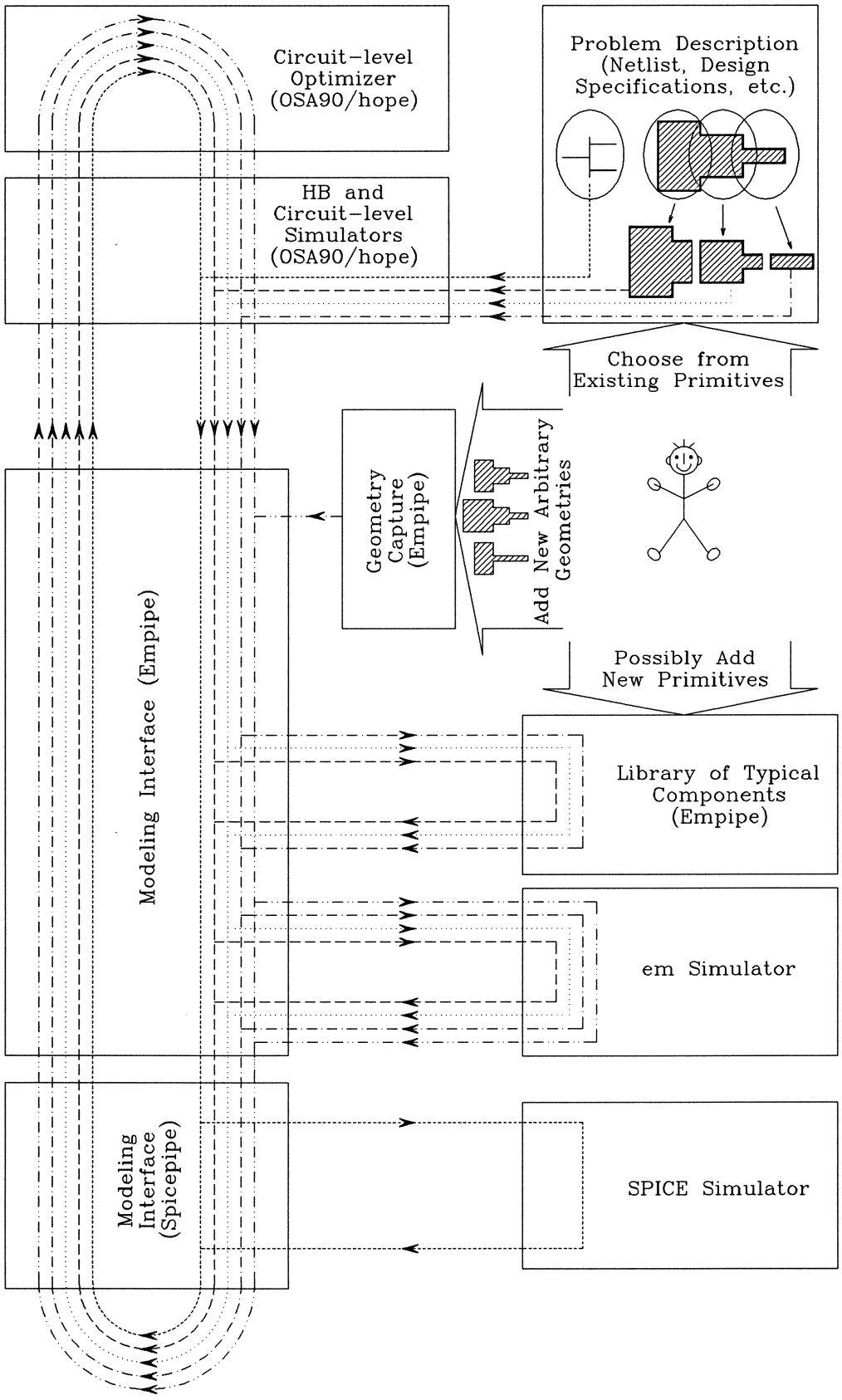

Bandler *et al.* "Optimization Technology ...", **Figure 6**

International Journal of Microwave and Millimeter-Wave Computer-Aided Engineering, vol. 7, no. 1, January 1997, Special Issue on Optimization-Oriented Microwave CAD.

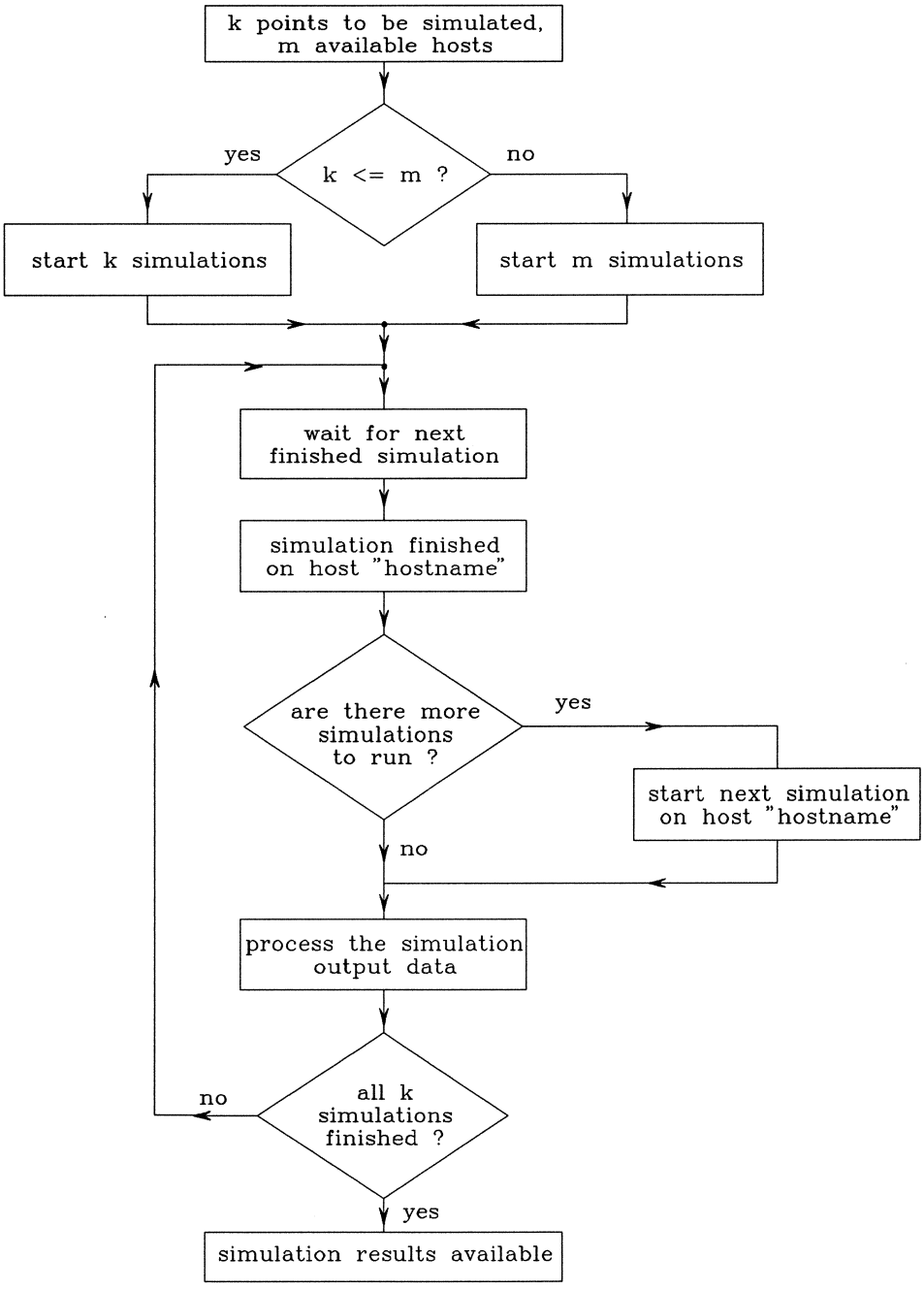

Bandler *et al.* "Optimization Technology ...", **Figure 7**

International Journal of Microwave and Millimeter-Wave Computer-Aided Engineering, vol. 7, no. 1, January 1997, Special Issue on Optimization-Oriented Microwave CAD.

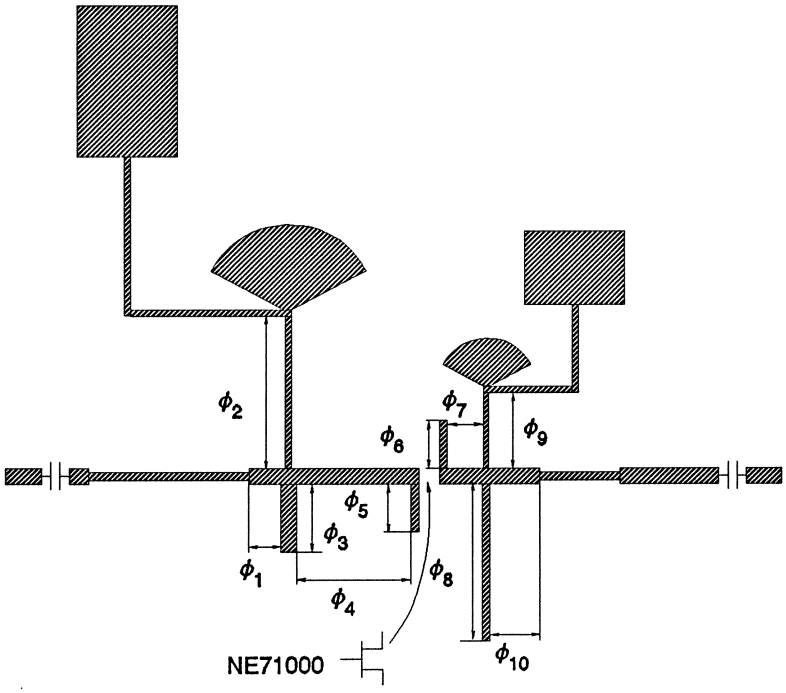

Bandler *et al.* "Optimization Technology ...", **Figure 8**

International Journal of Microwave and Millimeter-Wave Computer-Aided Engineering, vol. 7, no. 1, January 1997, Special Issue on Optimization-Oriented Microwave CAD.

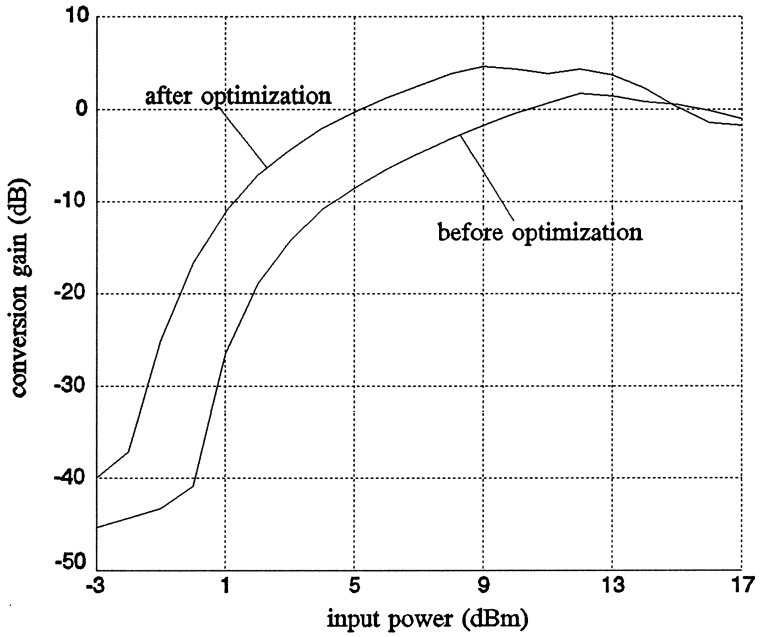

Bandler *et al.* "Optimization Technology ...", **Figure 9**

International Journal of Microwave and Millimeter-Wave Computer-Aided Engineering, vol. 7, no. 1, January 1997, Special Issue on Optimization-Oriented Microwave CAD.

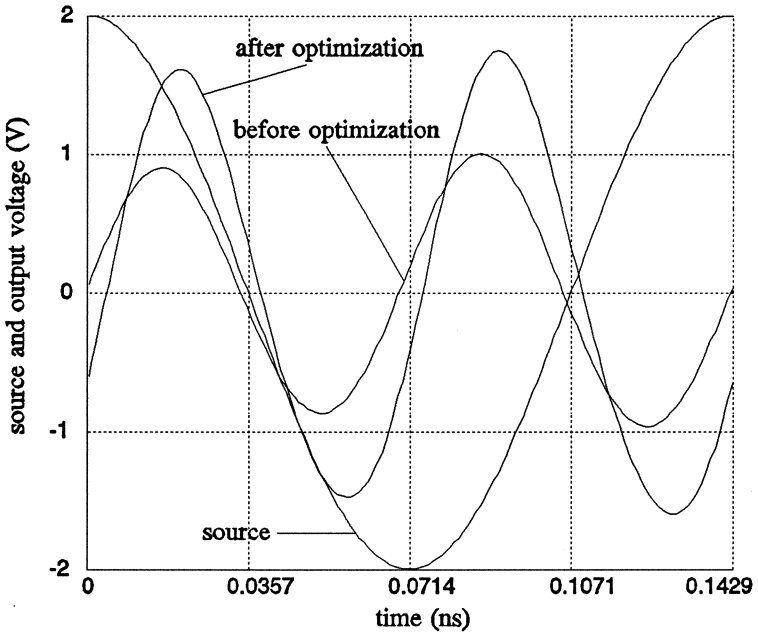

Bandler *et al.* "Optimization Technology ...", **Figure 10**

International Journal of Microwave and Millimeter-Wave Computer-Aided Engineering, vol. 7, no. 1, January 1997, Special Issue on Optimization-Oriented Microwave CAD.

(a)

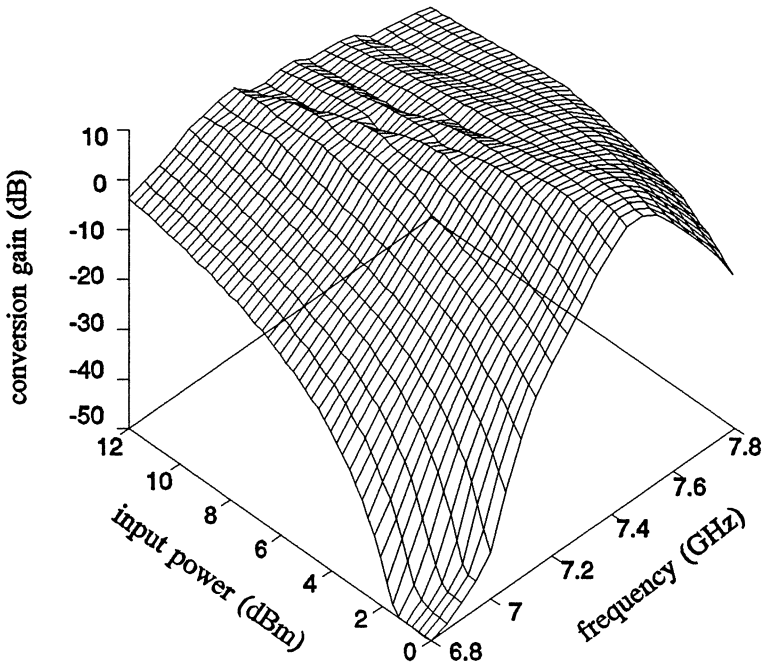

(b)

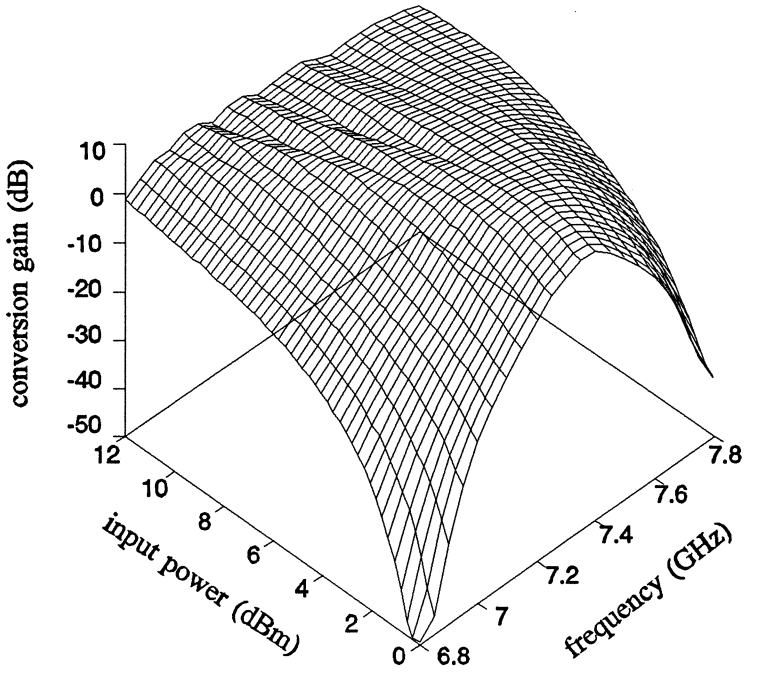

Bandler *et al.* "Optimization Technology ...", **Figure 11**

International Journal of Microwave and Millimeter-Wave Computer-Aided Engineering, vol. 7, no. 1, January 1997, Special Issue on Optimization-Oriented Microwave CAD.

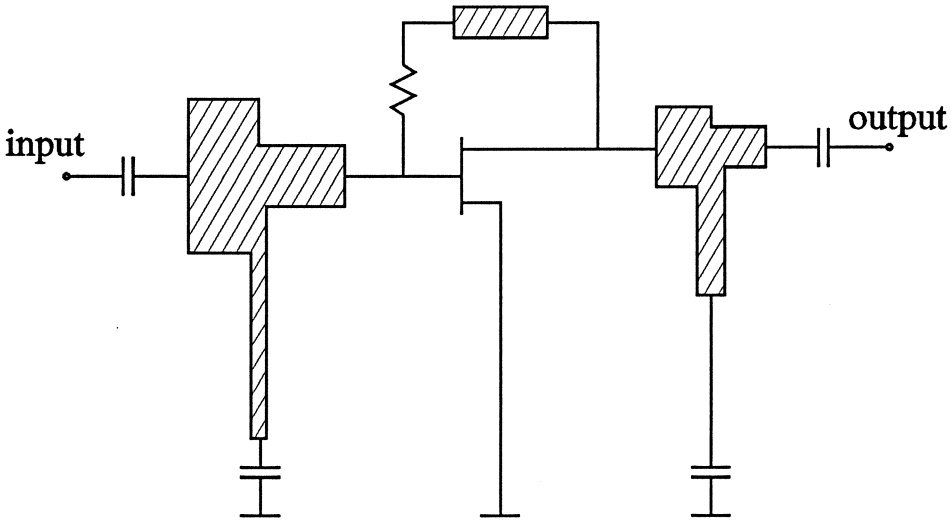

Bandler *et al.* "Optimization Technology ...", **Figure 12**

International Journal of Microwave and Millimeter-Wave Computer-Aided Engineering, vol. 7, no. 1, January 1997, Special Issue on Optimization-Oriented Microwave CAD.

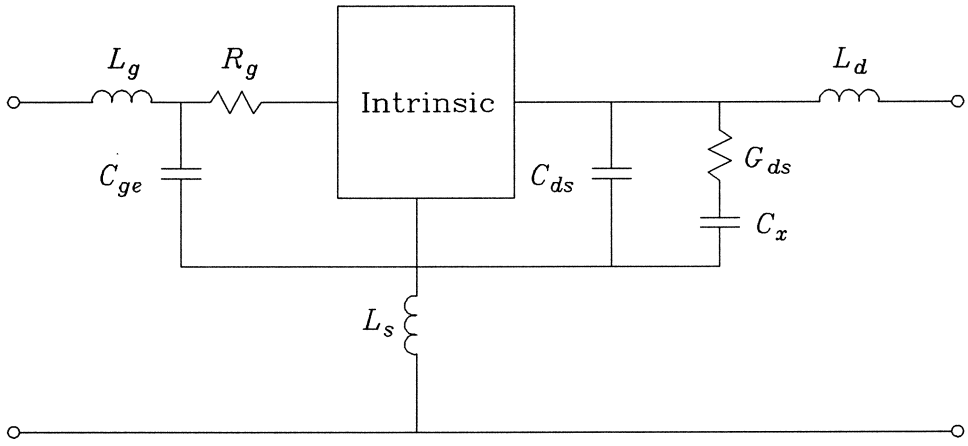

Bandler *et al.* "Optimization Technology ...", **Figure 13**

International Journal of Microwave and Millimeter-Wave Computer-Aided Engineering, vol. 7, no. 1, January 1997, Special Issue on Optimization-Oriented Microwave CAD.

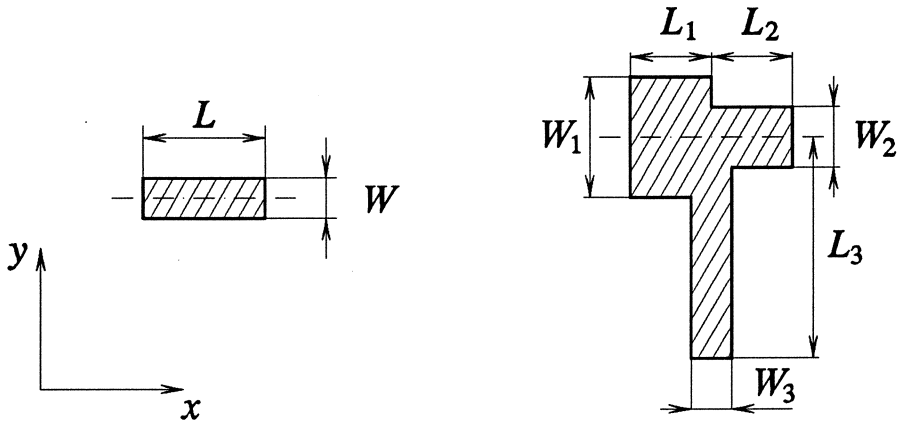

Bandler *et al.* "Optimization Technology ...", **Figure 14**

International Journal of Microwave and Millimeter-Wave Computer-Aided Engineering, vol. 7, no. 1, January 1997, Special Issue on Optimization-Oriented Microwave CAD.

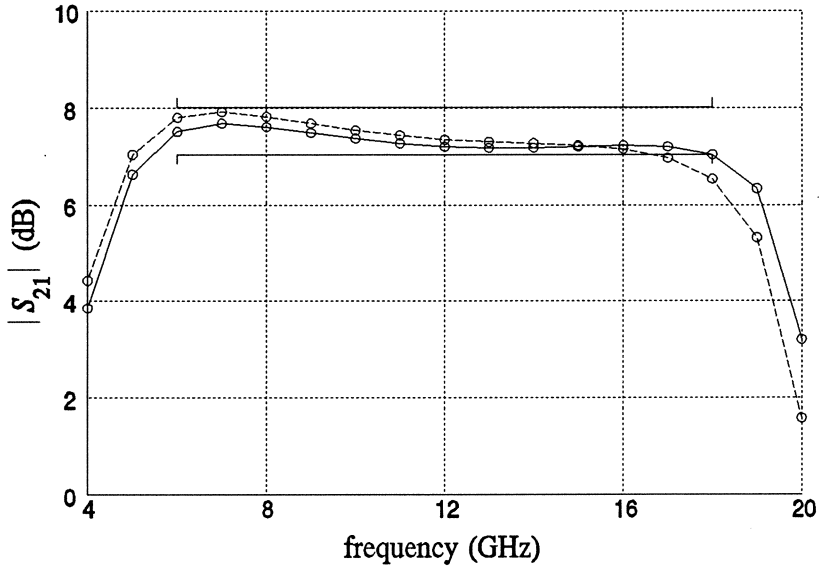

Bandler *et al.* "Optimization Technology ...", **Figure 15**

International Journal of Microwave and Millimeter-Wave Computer-Aided Engineering, vol. 7, no. 1, January 1997, Special Issue on Optimization-Oriented Microwave CAD.

(a)

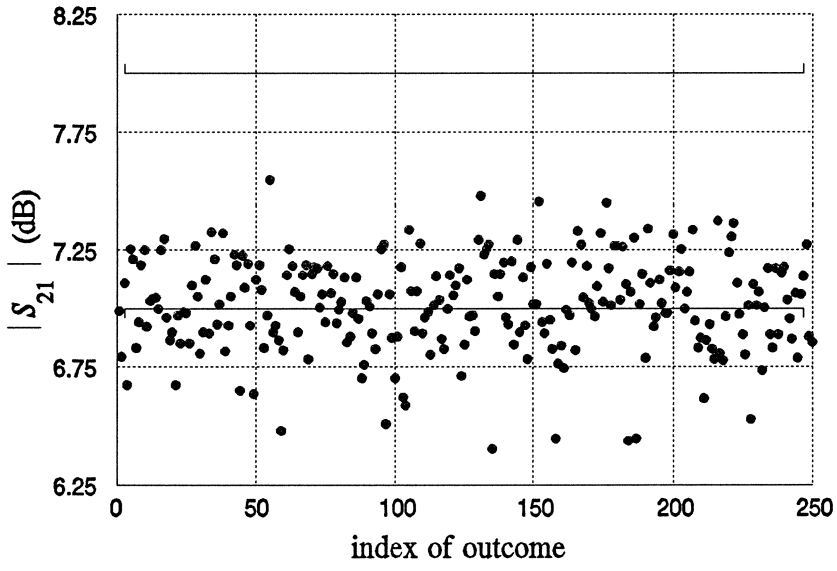

(b)

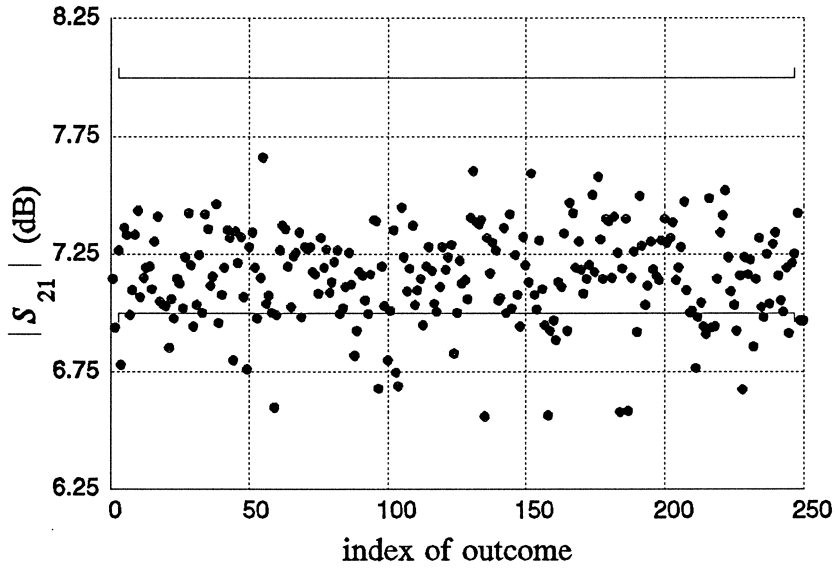

Bandler *et al.* "Optimization Technology ...", **Figure 16**

International Journal of Microwave and Millimeter-Wave Computer-Aided Engineering, vol. 7, no. 1, January 1997, Special Issue on Optimization-Oriented Microwave CAD.

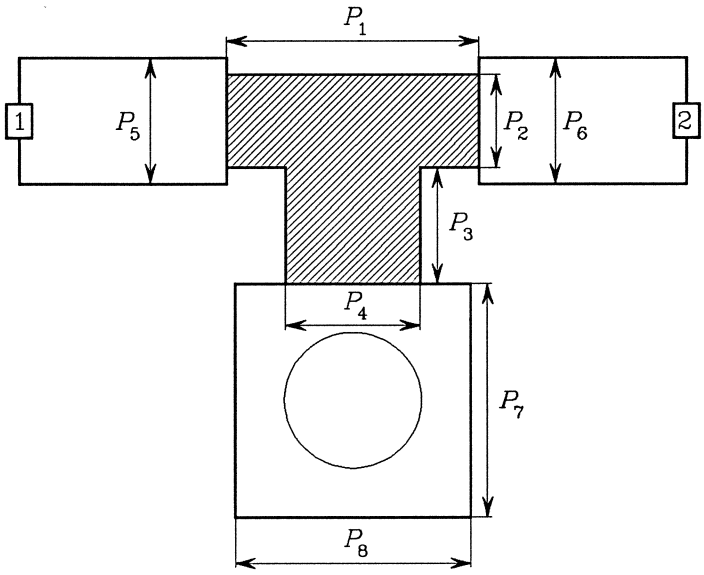

Bandler *et al.* "Optimization Technology ...", **Figure 17**

International Journal of Microwave and Millimeter-Wave Computer-Aided Engineering, vol. 7, no. 1, January 1997, Special Issue on Optimization-Oriented Microwave CAD.